ROTOR DYNAMICS ANALYSIS AND BEARING OPTIMIZATION STUDY OF A 3800 HP STEAM TURBINE

by

Dana J. Salamone

Chief Engineer

Centritech Corporation

Houston, Texas

Dana J. Salamone is Chief Engineer for Centritech Corporation in Houston, Texas. In this capacity, he is a bearing designer and consultant to the utility, marine, and petrochemical industries for the solution of turbomachinery vibration problems. He has eight years of industrial experience in stress analysis, structural vibrations, and rotor dynamics. Mr. Salamone received a Bachelor of Science in Mechanical Engineering (1974), and a Master of Science in Applied Mechanics (1977), from the University of Virginia. He is a member of ASME and has several ASME publications in the area of rotor dynamics. He is also a registered Professional Engineer in the State of Texas.

ABSTRACT

This paper presents the highlights of a complete rotor dynamics analysis and bearing optimization study that was performed on a 3800 HP multistage steam turbine. This unit is coupled to a three stage, poster-type, centrifugal air compressor with two high speed pinion shafts engaging a common bull gear. The turbine drives the lower speed pinion at a maximum speed of 10,500 rpm. Located at the other end of this same pinion is the first stage impeller wheel. The second and third stages are mounted on the higher speed pinion, rotating at a maximum speed of 13,600 rpm. The maximum speed of the bull gear is 1,940 rpm. All the existing compressor bearings are the four-lobe type.

The original turbine rotor consists of three stages and has a 41.34 inch bearing span. The bearings are lemon-bore type with journal diameters of 3.0 and 4.0 inches on the inlet and exhaust ends, respectively. This turbine has exhibited subsynchronous vibration, at approximately half rotational speed, during field testing. The half frequency vibration prevented operation above 9,400 rpm because a shaft resonance was excited and vibration levels became prohibitively high.

The analysis of the existing rotor-bearing system predicts that the turbine operates close to the second critical speed and that the rotor is stable under normal load conditions. However, the rotor becomes unstable when the lemon-bore bearings are unloaded.

There are two major sources of bearing load in addition to gravity. These loads are misalignment and gear mesh loading. Misalignment can result from differential thermal growth of the turbine and compressor cases and supports. If the coupling does not act as an ideal joint, this differential growth can impose external loads at the bearings. The bearing load resulting from the gear mesh is a reaction to the torque transmission at the gear interface. For example, the turbine driver rotates in the counter-clockwise direction. Therefore, the low speed pinion gear tends to climb up the bull gear, which causes an upward external load on the pinion bearings. As in the case of misalignment, if the coupling is not ideal, the turbine bearings can also be affected by these gear mesh reaction loads. This analysis is primarily concerned with the effect of these external loads that oppose gravity and cause degrees of net bearing unloading because the unloading causes rotor instability. The rotor is unstable with 75 pounds unloading at each bearing or 110 pounds unloading at the exhaust end bearing alone (with a normal gravity load at the inlet end bearing).

As a solution to the problem, a new set of bearings was designed to stabilize the rotor and move the peak response speeds away from the operating speed range. The new bearings are five-shoe-tilt-pad bearings with load-between-pad orientation. The inlet end bearing has a 3.0 inch diameter bore with length-to-diameter ratio of 1.0, and preload of 0.8. The exhaust end bearing has a 3.995 inch diameter bore with a length-to-diameter ratio of 0.4 and preload of 0.0.

With the new tilt-pad bearing design there are no response peaks in the normal operating speed range and the system log decrement is 2.8 times higher than with the existing system, under normal load conditions. The log decrement for the tilt-pad bearings is +0.52 for an unloading of 100 pounds. Therefore, the tilt-pads provide a stable rotor support that is not sensitive to unloading.

INTRODUCTION

The subject machine, shown in Figure 1, is a 3,800 HP steam turbine with a governor speed range of 8,000 to 10,500 rpm. The rotor is supported in two lemon-bore journal bearings, which are separated by a 41 inch bearing span. The inlet-end bearing has a 3.0 inch journal diameter, preload of 0.5, and

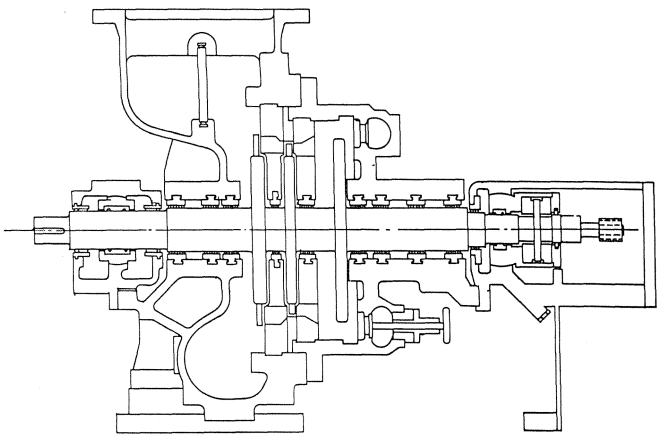

Figure 1. Three State Steam Turbine.

length-to-diameter ratio of 0.33. The exhaust end bearing has a 4.0 journal diameter, preload of 0.5, and length-to-diameter ratio of 0.25. The 490 pound rotating element consists of three turbine wheels with weights of 94, 61, and 76 pounds. The turbine drives a three stage, poster-type, air compressor with two high speed pinion shafts engaging a common bull gear, as schematically shown in Figure 2. The turbine is directly coupled to one end of the low speed pinion shaft by a 76 pound flexible coupling. Mounted on the other end of this same shaft is the 207 pound, first stage impeller. The total low speed pinion weight is 637 pounds. This shaft is supported in two four-lobe bearings with journal diameters of 4.724 and 5.906 inches at the coupling and impeller ends, respectively. The pinion engages the bull gear near the middle of its 22 inch bearing span.

The bull gear shaft is a 2,735 pound rotor, including a 2,522 pound bull gear mounted at the center of the 18 inch bearing span. The shaft is supported in two 5.906 inch diameter, four-lobe bearings. The maximum bull gear operating speed is 1,940 rpm.

The third compressor shaft is the high speed pinion shaft, which weighs 408 pounds. This shaft has a 93 pound, second stage impeller at one end and a 63 pound, third stage impeller at the other end. This pinion rotates at a maximum speed of 13,600 rpm. The shaft is supported in two 4.724 inch diameter, four-lobe bearings with a 22 inch bearing span.

The air compressor and turbine driver unit have exhibited high vibration levels that prohibit continuous operation. Vibration data was recorded in the field to identify vibration levels and dominant frequencies of the system. A strong synchronous vibration at a frequency of 175 Hz (10,500 rpm) was found throughout the compressor system. In addition, the turbine exhibited high subsynchronous vibration at approximately half rotational speed. Figure 3 is a cascade plot[1] showing the

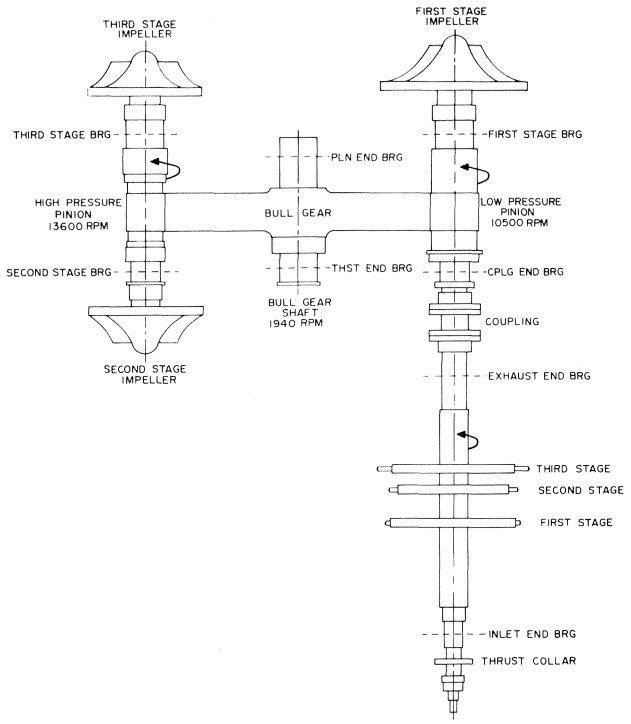

Figure 2. Turbine/Compressor Unit.

[1]This data courtesy of Mr. John S. Mitchell, consultant.

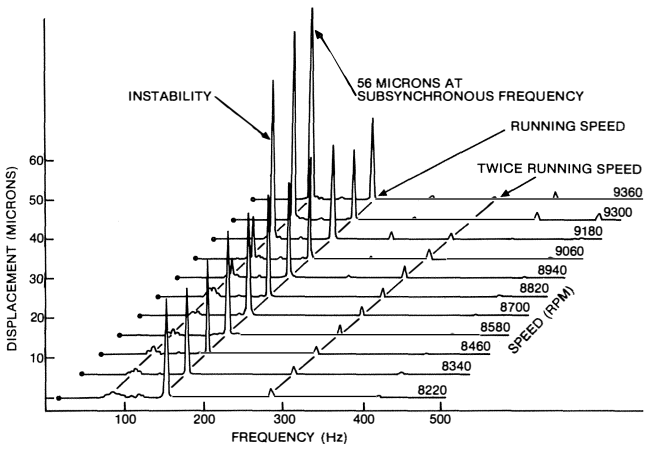

Figure 3. Cascade Plot.

frequency spectra for the turbine as it comes up to speed during an actual test run. As shown in the figure, this half frequency vibration tracked with running speed within the governor speed range, starting at approximately 8,000 rpm. As running speed was increased, the half frequency vibration increased in magnitude, limiting safe operation to speeds below 9,400 rpm. The high vibration at 9,400 rpm corresponds to the excitation of the first shaft resonance by the half.frequency component.

A complete rotor dynamics analysis was performed on the turbine and compressor rotor systems in order to determine the sources of these high vibrations and to identify a solution to the problem. The analysis results indicated specific dynamic problems in both the compressor and the turbine.

The compressor analysis revealed that the pinion and bull gear shafts had natural frequencies that coincided with the rotating speeds of the system. The implication is that the rotating speed of one shaft could excite the natural frequency of the other shafts and vice versa. As a result of the compressor study, a new set of bearings was designed to minimize this cross-excitation and to improve the synchronous vibration characteristics.

ROTOR SHAFT MODEL

Figure 5 shows the computer model indicating the division of the turbine rotor shaft into discrete sections. The rotor shaft is modeled as a series of lumped mass stations, containing the weights and inertia properties of the turbine wheels, oil deflectors, coupling, thrust collar, etc. These mass stations are mathematically interconnected by elastic shaft elements. The model also includes the bearing support locations to incorporate speed-dependent stiffness and damping properties of the oil film. Figure 4 illustrates two of the new compressor bearing assemblies.

The analysis of the turbine rotor determined that it was unstable if the lemon-bore bearings were unloaded. The results of the turbine analysis and the subsequent bearing optimization study are the focal point of this paper.

UNDAMPED CRITICAL SPEEDS

Critical Speed Map

Figure 6 is a critical speed map for a typical multimass rotor. The map is a plot of the first three undamped critical speeds versus a range of arbitrarily selected bearing stiffness

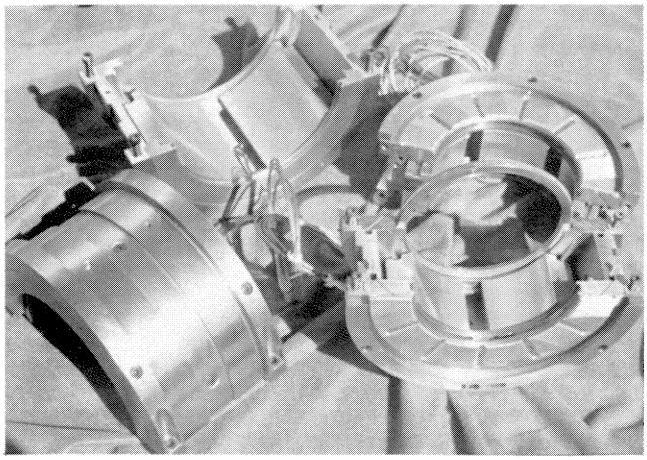

Figure 4. New Compressor Bearing Assemblies.

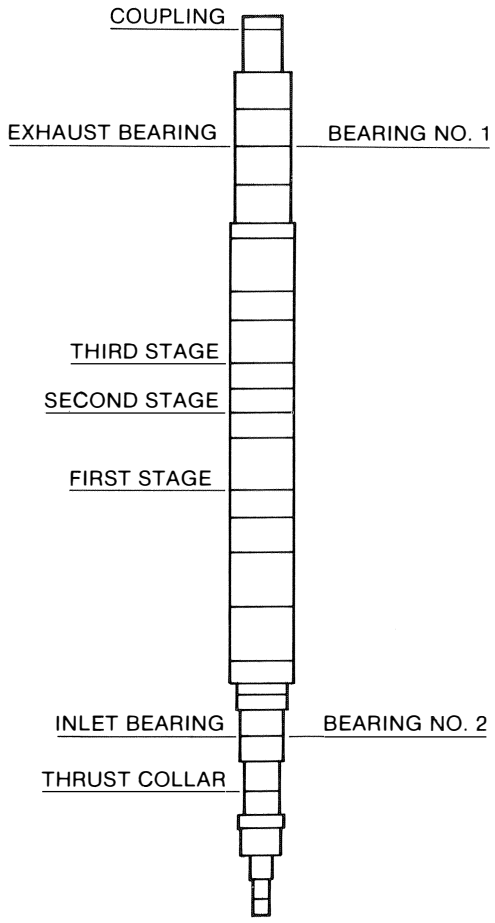

Figure 5. Shaft Cross Section Computer Model.

values. The critical speeds increase as the stiffness of the bearings are increased. However, these curves all become asymptotic to an upper limiting speed. In this region, the critical speeds are insensitive to increasing bearing stiffness and the bearing damping is no longer effective for the suppression to vibration.

The actual critical speed map for the turbine rotor model

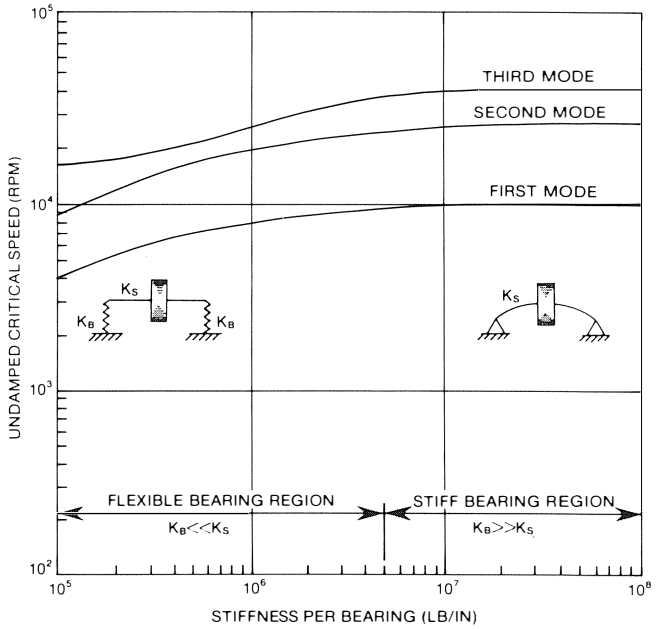

Figure 6. Typical Undamped Critical Speed Map.

is shown in Figure 7. Note the proximity of the 10,500 rpm operating speed to the second and third critical speeds. The first critical speed (first mode) has a rigid bearing limit of 6,594 rpm.

Mode Shapes

The rotor mode shapes indicate the relative rotor amplitudes at the undamped critical speeds. The locations of maximum relative amplitude would be sensitive to unbalance, whereas the node points would not. The mode shapes also indicate the amount of motion at the bearing locations.

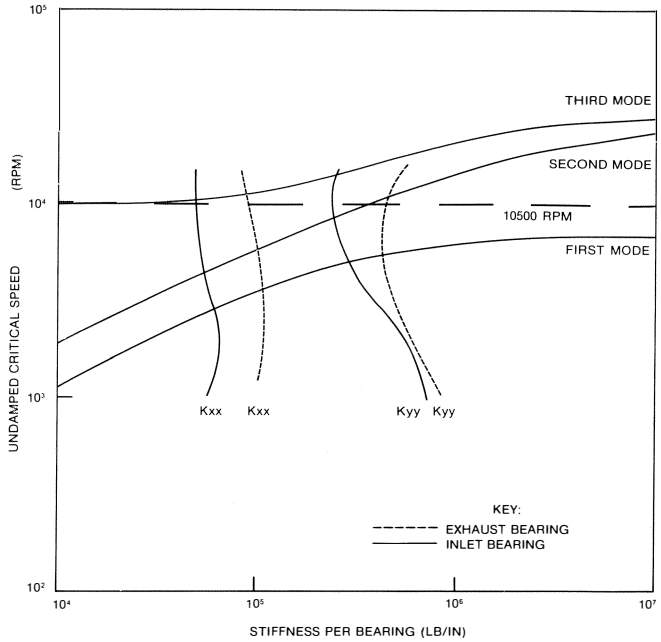

Figure 7. Undamped Critical Speed Map Steam Turbine Rotor Lemon Bore Bearings.

Figures 8 through 10 are undamped critical speed mode shapes for the turbine rotor considering bearing stiffness values of $1x10^5$, $1x10^6$, and $1x10^7$ lb/in. The two bearings are assigned the same stiffness values, as indicated in the figure title. Note that figures 8a and 8b show very little rotor bending, because a bearing stiffness of $1x10^5$ lb/in is quite flexible compared to the rotor shaft stiffness. For this bearing stiffness case, the first and second modes are cylindrical and conical modes, respectively, with a great deal of bearing motion. If the bearing stiffnesses were increased to $1x10^6$ lb/in (Figure 9), there is considerably more rotor bending than in the previous case and there is still some motion at the bearings to provide damping forces. Therefore, the bearings appear stiffer relative to the shaft, but are not yet rigid. Finally, if the bearing stiffnesses are further increased to $1x10^7$ lb/in (Figure 10), there is no bearing motion. This represents the rigid bearing case where the bearings are far too stiff for the rotor. In this condition, the rotor has no effective bearing damping because there is no bearing motion. Referring to the critical speed map, this condition would occur at bearing stiffnesses above $2x10^6$ lb/in. Therefore, an alternate bearing design must not exceed this bearing stiffness value at the first critical speed, in order to allow safe operation through this mode.

ORIGINAL LEMON BORE BEARINGS

Description

The original bearings, shown schematically in Figure 11, are lemon-bore bearings. The inlet-end bearing has a 3.0 inch journal diameter, a length of 0.98 inches, preload of 0.5, and an average running clearance of 0.005 inches. The exhaust end bearing has a journal diameter of 3.995 inches, a length of 0.98 inches, a preload of 0.5, and an average running clearance of 0.004 inches. The lubricating oil is rated at 240 ssu @ 100°F. This oil has an absolute viscosity of $2.02x10^{-6}$ reyns at 150°F.

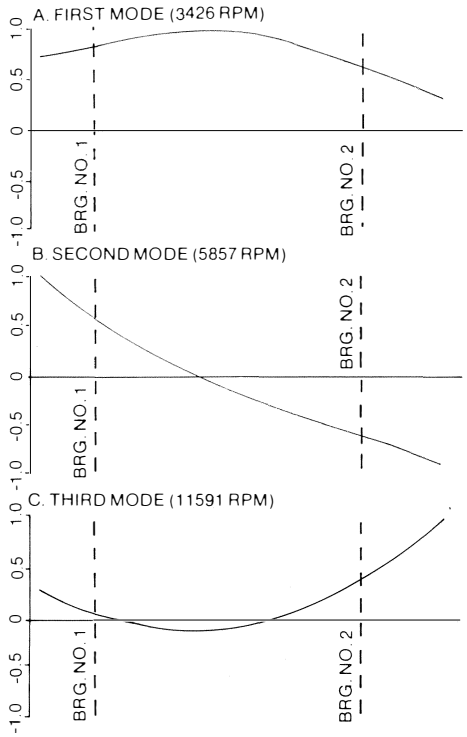

Figure 8. Mode Shapes Bearing Stiffness = 1 x 10^5 LB/IN.

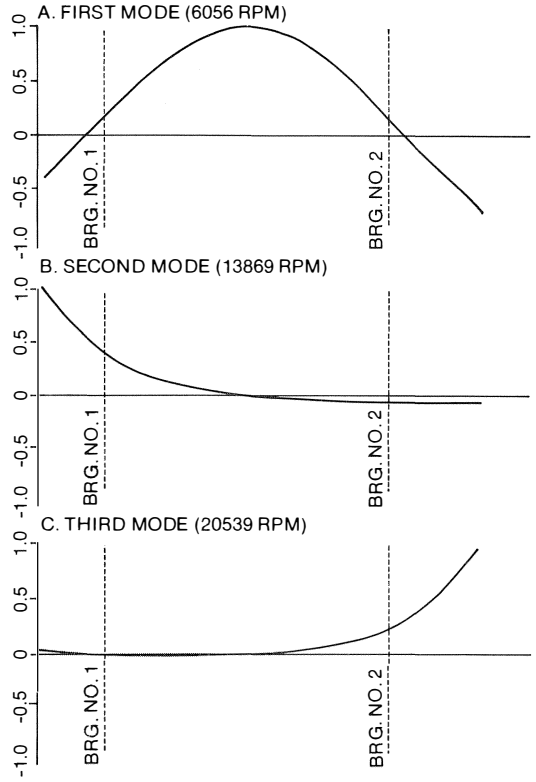

Figure 9. Mode Shapes Bearing Stiffness = 1 x 10^6 LB/IN.

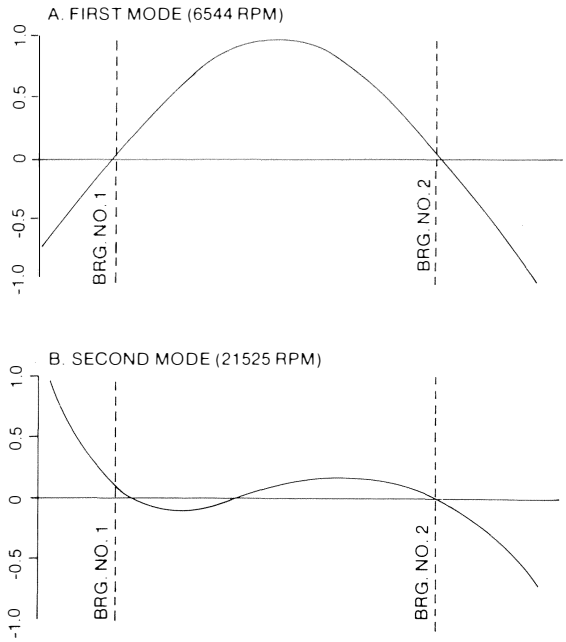

Figure 10. Mode Shapes Bearing Stiffness = 1 x 10^7 LB/IN.

Bearing Coefficients and Critical Speeds

The horizontal and vertical bearing stiffness coefficients for the lemon bore bearings are plotted on the map and are identified as X and Y, respectively. The intersections of these stiffness and critical speed curves are the predicted undamped

critical speeds. It can be seen that the principal stiffness values for these bearings intersect the second and third mode curves very close to the operating speed of 10,500 rpm. Table 1 lists these intersections, which are the undamped critical speeds. Note that the second critical vertical plane and third critical horizontal plane, are within and near the governor speed range of 8,000 to 10,500 rpm.

UNBALANCE RESPONSE IN LEMON-BORE BEARINGS

Unbalance Criteria

A synchronous unbalance response analysis identifies the peak response speeds and the magnitude of the rotor amplitudes. These results indicate the rotor sensitivity and the effectiveness of the bearing damping.

The rotor unbalance criteria used in this analysis consists of the following:

1. In-Phase: 10% of the rotor weight distributed equally among the turbine wheels ($\phi = 90°$)
2. Out-of-Phase couple at rotor ends:
   a) 10% of bearing No. 1 load at the third stage wheel ($\phi = 0°$)
   b) 10% of bearing No. 2 load at the first stage wheel ($\phi = 180°$)
3. Coupling: Ten times the Navy standard
   $10 \times (4W_{cplg}/N)$ ($\phi = 90°$)
4. Thrust collar: One mil eccentricity ($\phi = 270°$)

Note: ϕ indicates phase angle orientation

Response Plots

Figures 12 through 14 are the predicted unbalance response amplitude plots for the turbine rotor in lemon bore bearings. These amplitudes should only be used for relative comparison purposes, since they are dependent on the assumed amount and location of the unbalance. It should also be noted that these calculations assume that the bearings are supported by a rigid casing and base. Table 2 lists the peak response amplitudes and speeds corresponding to the excitation of the critical speeds. The peak responses at 8,760 to 12,530 rpm are of particular interest because they lie in and near the governor speed range of 8,000 - 10,500 rpm. These higher speed peak responses result from excitation of the second critical speed of the turbine.

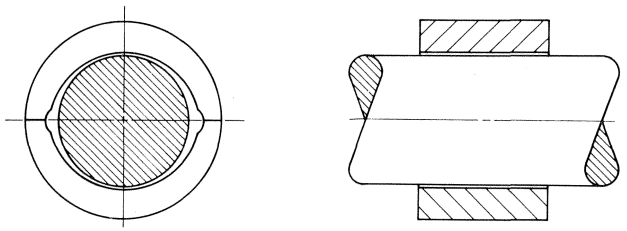

Figure 11. Lemon Bore Bearing.

TABLE 1. UNDAMPED CRITICAL SPEEDS OF A STEAM TURBINE ROTOR WITH LEMON-BORE BEARINGS.

Critical	Horizontal Plane	Vertical Plane
First	3,200 rpm	5,100 rpm
Second	5,200 rpm	9,500 rpm
Third	10,900 rpm	16,400 rpm

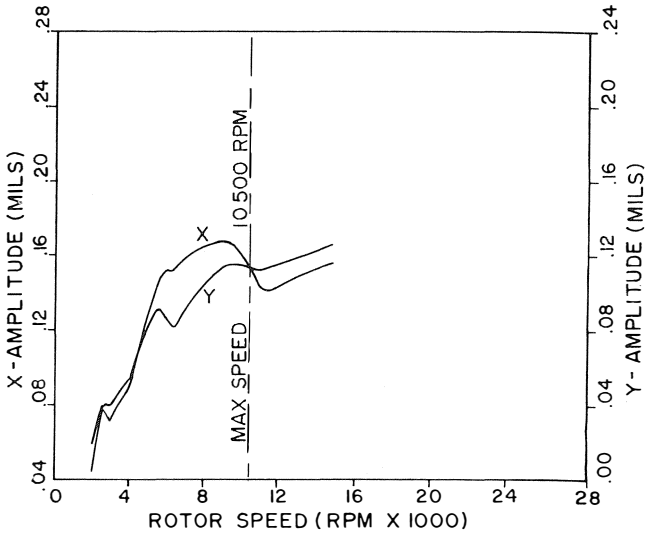

Figure 12. Unbalance Response Amplitudes Lemon Bore Bearings Exhaust End BRG Location.

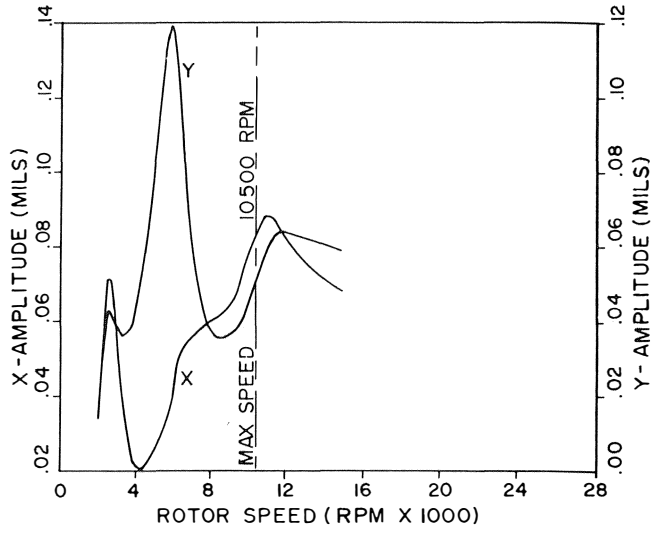

Figure 13. Unbalance Response Amplitudes Lemon Bore Bearings Rotor Center Location.

STABILITY WITH LEMON-BORE BEARINGS

Bearing Stability

There are two major sources of bearing load in addition to gravity. These loads are misalignment and gear mesh loading. Misalignment can result from differential thermal growth of the turbine and compressor cases and supports. If the coupling does not act as an ideal joint, this differential growth can

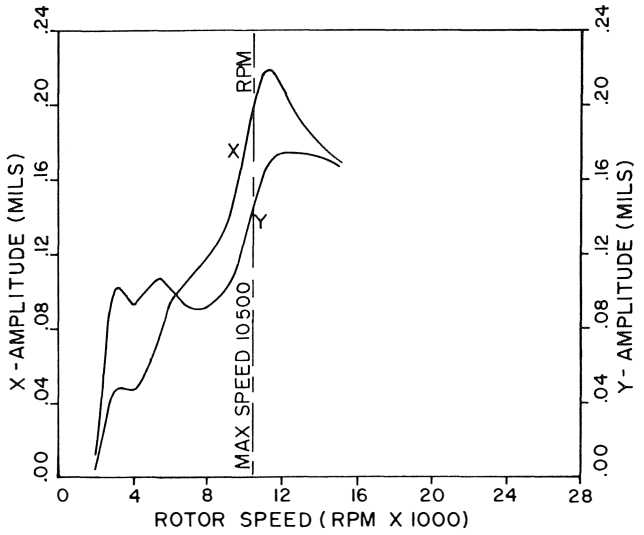

Figure 14. Unbalance Response Amplitudes Lemon Bore Bearings Inlet End BRG Location.

TABLE 2. PEAK RESPONSE SPEEDS AND AMPLITUDES OF A STEAM TURBINE ROTOR WITH LEMON-BORE BEARINGS*.

	SHAFT LOCATION			
Plane	Coupling	Exhaust Bearing	Center Wheel	Inlet Bearing
Horizontal	2500 (0.07)	2500 (0.07)	2600 (0.06)	2800 (0.07)
Vertical	2600 (0.03)	2600 (0.03)	2700 (0.04)	2900 (0.03)
Horizontal	5900 (0.20)	6160 (0.15)	No Peak	5380 (0.11)
Vertical	5250 (0.08)	5640 (0.09)	5900 (0.12)	6160 (0.10)
Horizontal	8760 (0.21)	8890 (0.17)	11,100 (0.09)	11,230 (0.22)
Vertical	8760 (0.15)	9670-9800 (0.12)	12,010 (0.06)	12,400-12,530 (0.17)

*NOTE: Tabulated values are peak response speeds in rpm. Bracketed values are peak amplitudes in mils.

impose external loads at the bearings. The bearing load resulting from the gear mesh is a reaction to the torque transmission at the gear interface. For example, the turbine driver shown in Figure 2 rotates in the counter-clockwise direction. Therefore, the low speed pinion gear tends to climb up the bull gear, which causes an upward external load on the pinion bearings. As in the case of misalignment, if the coupling is not ideal, the turbine bearings can also be affected by these gear mesh reaction loads. This analysis is primarily concerned with the effect of these external loads that oppose gravity and cause degrees of net bearing unloading.

Figure 15 is a plot of bearing stability margin versus bearing unloading at operating speed. Note that at zero unloading, which is the normal gravity load case, the bearings are stable by 18 and 31% margins at the inlet and exhaust ends, respectively. However, both bearings become unstable for 75

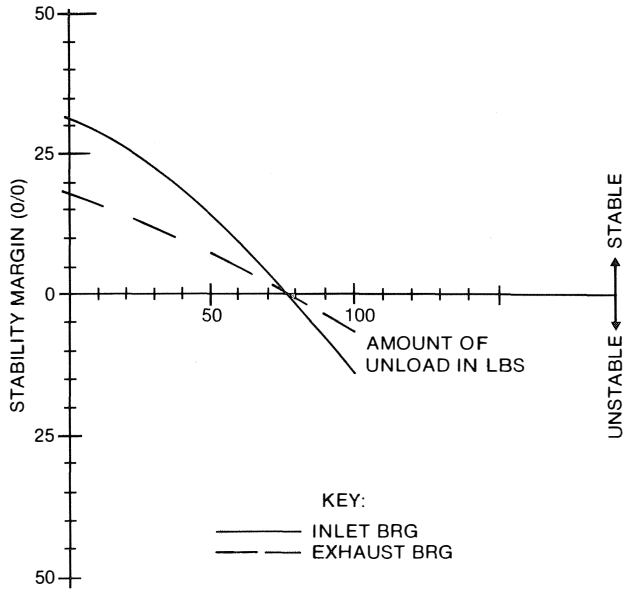

Figure 15. Bearing Stability Versus Unloading Force Lemon Bore Bearings Operating Speed 10600 RPM.

pounds of unloading. Therefore, either bearing can go unstable if a gear load or misalignment-induced load is transmitted through the coupling to lift the journal with a force of only 75 pounds. This presents a potential rotor stability problem.

Flexible Rotor Stability

Flexible rotor stability is assessed by calculating the damped eigenvalues for the rotor and bearing system. The damped eigenvalue ($s = \lambda + i\omega$) is a complex number composed of a real part (λ), which is the growth factor and an imaginary part (ω), which is the damped natural frequency. The growth factor is the rate of exponential decay or growth of the vibration amplitudes. If λ is positive, the vibration grows with time and the system is unstable. If λ is negative, the vibration decays with time and the system is stable.

The log decrement (δ) is a standard non-dimensional indicator of stability of a system. It represents the natural log of the ratio of two successive amplitudes of system vibration and is computed from the complex eigenvalue as $\delta + -2\pi\lambda/\omega$. If δ is positive, the system is stable. If δ is negative, the system is unstable.

Table 3 lists the flexible rotor stability results. Note that the rotor is stable for normal design loads (zero bearing unloading). In this case, the log decrement is +0.19. However, for a

TABLE 3. FLEXIBLE ROTOR STABILITY VERSUS BEARING UNLOADING OF A STEAM TURBINE ROTOR WITH LEMON-BORE BEARINGS AT OPERATING SPEED 10,600 RPM.

Unloading at Each Bearing (lb)	Damped Frequency (rpm)	Log Decrement	Condition
0	3700	+0.19	Stable
50	3560	+0.07	Stable
75	3460	−0.02	Unstable

75 pounds unloading at each bearing, the system is unstable, with a log decrement of −0.022. Therefore, this system has a potential stability problem that can result when the bearings become unloaded by transmitted coupling forces.

This problem was further pursued by considering unloading only at the exhaust end bearing, because it lies at the coupling end of the machine. For this case, it was assumed that the inlet end bearing had a normal gravity loading. Figure 16 is a plot of rotor stability versus unloading at the exhaust-end bearing. It was found that a 110 pounds unloading force at the exhaust bearing would put the rotor on the stability threshold.

SUMMARY OF EXISTING SYSTEM

This analysis shows that the present rotor system, with the existing lemon bore bearings, has peak response amplitudes that occur within the governor speed range of 8,000 to 10,500 rpm. These responses result from excitation of the second critical speed.

In addition, the turbine rotor system is unstable for only 75 pounds unloading at each bearing or 110 pounds at the exhaust-end bearing alone. This rotor instability occurs because the lemon-bore bearings become unstable when they are unloaded. Therefore, it was necessary to find an alternate bearing design to eliminate this potential instability. These results were of particular concern because an instability was observed in field testing.

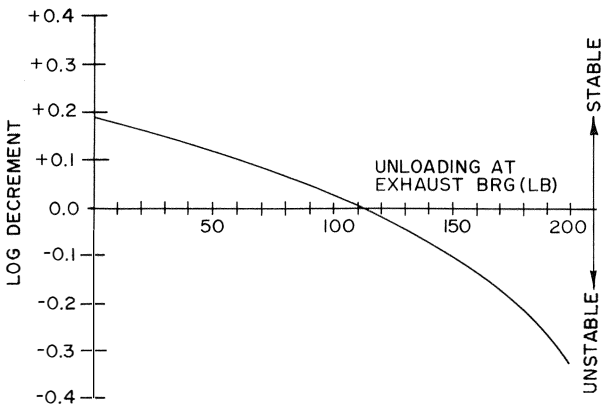

Figure 16. Flexible Rotor Stability Versus Unloading at Exhaust End Bearing.*

NEW BEARING CONVERSION

Description

The new turbine bearing conversion is shown in Figure 17. The journal bearings are five-shoe-tilting-pad bearings oriented with load-between-pad. The inlet-end bearing has a 3.0 inch diameter journal, a 0.8 preload, and a 3.0 inch pad length. The exhaust-end bearing has a 3.995 inch journal diameter, a 0.0 preload, and a 3.2 inch pad length. Figure 18 is a photograph of the new conversion assembly hardware.

Bearing Coefficients

The stiffness coefficients for the new tilt pad bearings are shown on the critical speed map for the existing rotor in Figure 19. In order to quantify the undamped critical speeds, it was more convenient to average the inlet and exhaust bearing stiffness characteristics in the horizontal and vertical planes. These average stiffness curves are also shown in Figure 19.

Table 4 lists the intersections of the new bearing and critical speed curves, which represent the approximate undamped critical speeds with the new tilt-pad bearings. The table shows that there are no undamped critical speeds in the governor speed range.

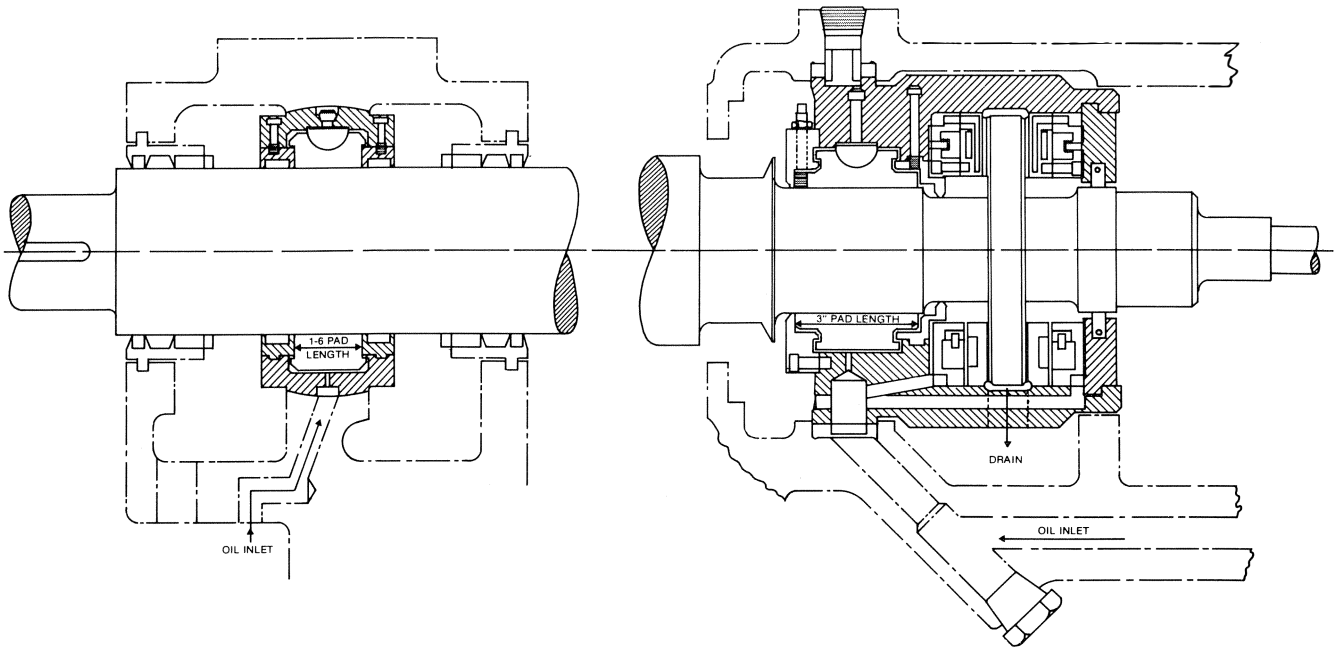

Figure 17. New Tilt Pad Bearing Conversion for Existing Rotor Shaft.

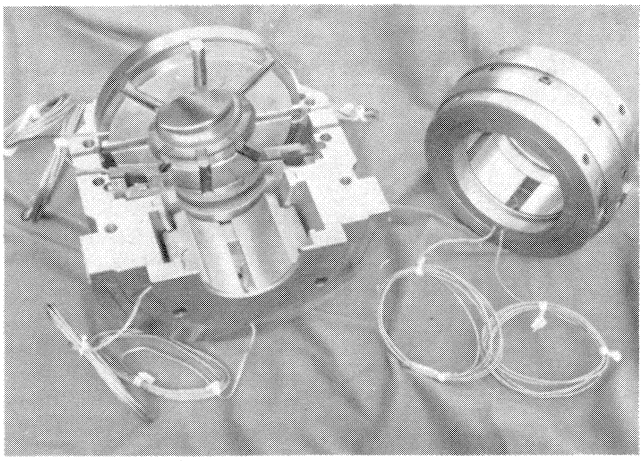

Figure 18. New Conversion Assembly Hardware.

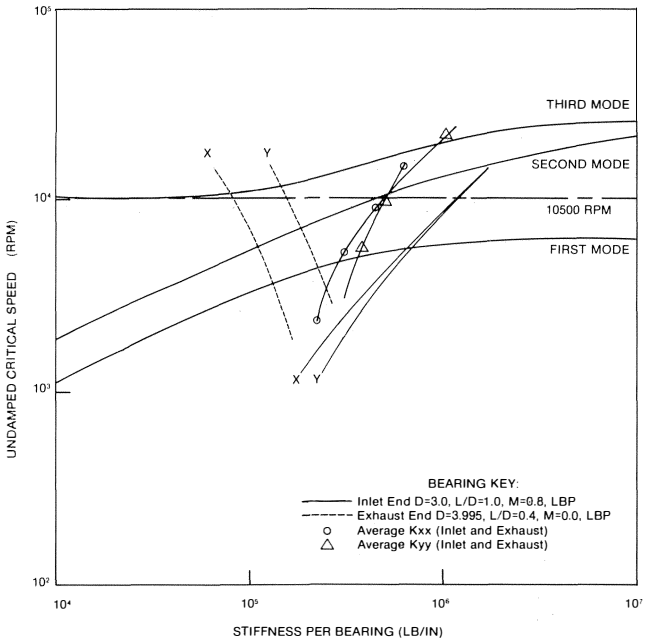

Figure 19. Undamped Critical Speed Map Steam Turbine Rotor New Tilt Pad Bearings.

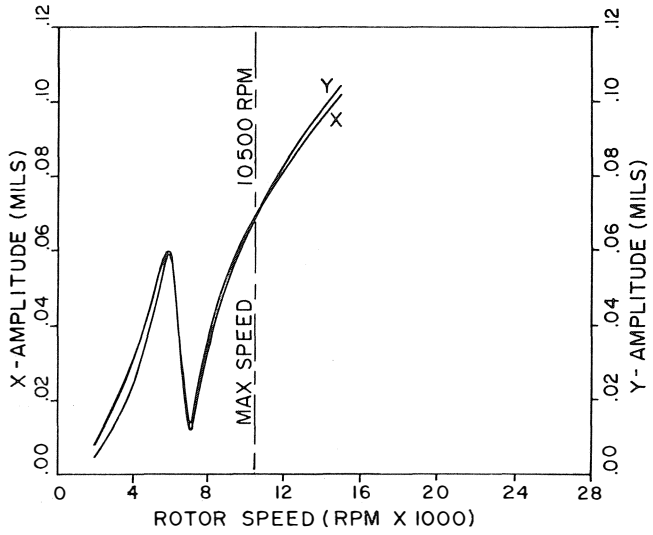

Figure 20. Unbalance Response Amplitudes Tilt Pad Bearings Exhaust End BRG Location.

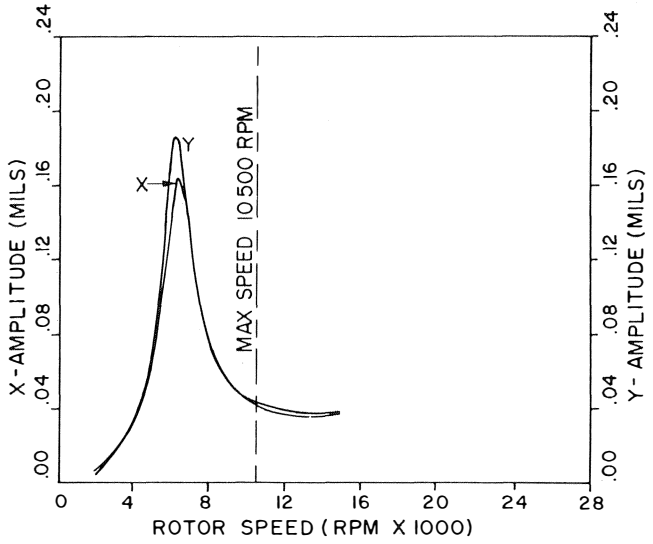

Figure 21. Unbalance Response Amplitudes Tilt Pad Bearings Rotor Center Location.

TABLE 4. UNDAMPED CRITICAL SPEED OF A STEAM TURBINE ROTOR WITH NEW TILT-PAD BEARINGS.

	Horizontal	Vertical
First Critical	5,000 rpm	5,200 rpm
Second Critical	12,000 rpm	12,200 rpm

UNBALANCE RESPONSE IN NEW TILT PAD BEARINGS

Response Plots

Figures 20 through 22 are the predicted unbalance response amplitudes versus rotor speed with the new tilt-pad bearings. Note the position of the maximum operating speed, indicated on the amplitude plots, relative to the peak amplitudes. Table 5 summarizes the peak response speeds and amplitudes with these new tilt-pad bearings. Note that only one peak response is observed between 5,900 and 6,550 rpm. Therefore, there are no peaks in the governor-operating-speed range with the new bearing design.

STABILITY WITH NEW TILT PAD BEARINGS

Bearing Stability

The tilt pad bearing is an inherently stable bearing because the cross-coupled stiffness coefficients, which cause instability, are essentially negligible compared to the principle stiffness terms.

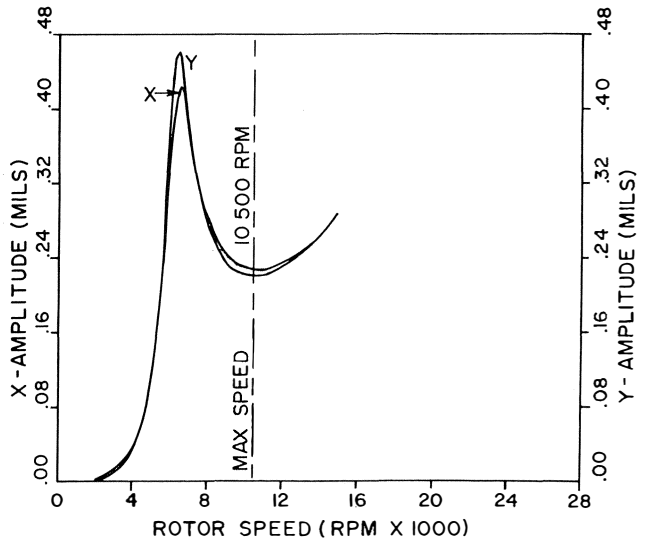

Figure 22. Unbalance Response Amplitudes Tilt Pad Bearings Inlet End BRG Location.

TABLE 5. PEAK RESPONSE SPEEDS AND AMPLITUDES OF A STEAM TURBINE ROTOR WITH NEW TILT-PAD BEARINGS*.

		Shaft Location		
Plane	Coupling	Exhaust Bearing	Center Wheel	Inlet Bearing
Horizontal	No Peak	5900 (0.06)	6420 (0.16)	6550 (0.04)
Vertical	No Peak	5900 (0.06)	6290 (0.19)	6420 (0.05)
— No Other Peaks up to 14,870 RPM —				

*NOTE: Tabulated values are peak response speeds in rpm. Bracketed value are peak amplitudes in mils.

Flexible Rotor Stability

Table 6 indicates the flexible rotor stability versus bearing unloading for the new tilt-pad bearings. Note that the system is stable for the design load condition (zero bearing unloading). The system remains very stable even with a 100 pounds unloading at each bearing. Therefore, the system stability is not sensitive to bearing unloading due to transmitted gear loads and misalignment-induced load with the new bearing design.

CONCLUSIONS

1. The turbine rotor with the existing lemon-bore bearings has undamped critical speeds within and near the governor speed range of 8,000 to 10,500 rpm. Specifically, there is a second undamped critical speed in the vertical plane at 9,500 rpm and a third undamped critical speed in the horizontal plane at 10,900 rpm.

TABLE 6. FLEXIBLE ROTOR STABILITY VERSUS BEARING UNLOADING — NEW TILT PAD BEARINGS AT OPERATING SPEED 10,500 RPM.

Unloading at Each Bearing (lb)	Frequency (rpm)	Log Decrement	Condition
0	6,220	+0.54	Very Stable
100	6,280	+0.52	Very Stable

2. The unbalance response analysis for the existing system indicates peak responses in the governor speed range. These peak responses occur between 8,760 and 12,530 rpm and result from excitation of the second critical speed.
3. The turbine with the existing lemon-bore bearings is stable with a normal gravity loading at the bearings. However, the rotor is unstable with 75 pounds unloading at each bearing or 110 pounds unloading at the exhaust-end bearing alone (with a normal gravity load at the inlet-end bearing).
4. A new set of bearings was designed to stabilize the rotor and move the peak response speeds away from the operating speed range. The new bearings are five-shoe-tilt-pad bearings with load-between-pad orientation. The inlet end bearing has a 3.0 inch diameter bore with length-to-diameter ratio of 1.0, and preload of 0.8. The exhaust end bearing is 3.995 inch diameter bore with a length-to-diameter ratio of 0.4, and preload of 0.0.
5. With the new tilt-pad bearing design there are no response peaks in the normal operating speed range and the system log decrement is 2.8 times higher than with the existing system, under normal load conditions. The log decrement for the tilt-pad bearings is +0.52 for an unloading of 100 pounds. Therefore, the tilt-pads provide a stable rotor support that is not sensitive to unloading.

REFERENCES

1. Barrett, L. E., Gunter, E. J., and Allaire, P. E., "Optimum Bearing and Support Damping for Unbalance Response and Stability of Rotating Machinery," A.S.M.E. Paper No. 77-GT-27, March, 1977.
2. Gunter, E. J., "Dynamic Stability of Rotor-Bearing Systems," NASA SP-113, 1966.
3. Lund, J. W., "Stability and Damped Critical Speeds of a Flexible Rotor in Fluid Bearings," *Journal of Engineering for Industry*, Trans. ASME, May, 1974, pp. 509-517.
4. Gunter, E. J., and Trumpler, P. R., "The Influence of Internal Friction on the Stability of High Speed Rotors with Anisotropic Supports," *Journal of Engineering for Industry*, Trans. ASME, November, 1969, pp. 1105-1128.
5. Salamone, D. J., and Gunter, E. J., "Effects of Shaft Warp and Disk Skew on the Synchronous Unbalance Response of a Multimass Flexible Rotor in Fluid Film Bearings," *Topics in Fluid Film Bearing and Rotor Bearing System Design and Optimization*, ASME Book No. 100118, pp. 79-107, April, 1978.